Research Square

Preprints are preliminary reports that have not undergone peer review.
They should not be considered conclusive, used to inform clinical practice,
or referenced by the media as validated information.

Spontaneously immortalized porcine cells support scalable cultured pork production in serum-free suspension

Liang Zhao

liang.zhao@njau.edu.cn

Nanjing Agricultural University https://orcid.org/0000-0003-2446-5577

Guang-Hong Zhou

Nanjing Agricultural University, Nanjing, China

Shijie Ding

Nanjing Joes Future Food Technology Co. Ltd.

Huifang Li

Joes Future Food Technology Co. Ltd

Haozhe Zhu

Joes Future Food Technology Co. Ltd

Zhongyuan Wu

Joes Future Food Technology Co., Ltd

Yi Kuang

Joes Future Food Technology Co. Ltd

Bing Yue

Joes Future Food Technology Co. Ltd

Chunhua Jian

Joes Future Food Technology Co. Ltd

Chen Wang

Joes Future Food Technology Co. Ltd

Wei Li

Nanjing Agricultural University

Yunting Xie

Nanjing Agricultural University

Chunbao Li

Nanjing Agricultural University https://orcid.org/0000-0002-0708-891X

Changbo Tang

Nanjing Agricultural University

Article

Keywords:

Posted Date: November 4th, 2026

DOI: https://doi.org/10.21203/rs.3.rs-11402436/v1

License: This work is licensed under a Creative Commons Attribution 4.0 International License.
Read Full License

Additional Declarations:
Yes there is potential Competing Interest. H.L., H.Z., Z.W., Y.K., B.Y., C.J., C.W., W.L., and S.D. are employees of Joes Future Food Technology Co. Ltd, which developed the cell line and the culture media and participated in this study. All authors declare no other competing interests.

Porcine muscle tissues were obtained from a 1-week-old pig. All animal procedures complied with applicable animal welfare regulations and the guidelines of the Animal Ethics Committee of Nanjing Agricultural University, China. Procedures involving the pig were conducted in accordance with protocol NJAU-CAST-2011-093. Mouse experiments were conducted by Wuhan Canvest Biotechnology Co., Ltd. under a protocol approved by the Animal Ethics Committee of Nanjing Agricultural University (approval no. NJAULLSC2024057).

Spontaneously immortalized porcine cells support scalable cultured pork production in serum-free suspension

Huifang Li[1,4], Haozhe Zhu[1,4], Zhongyuan Wu[1,4], Yi Kuang[1], Bing Yue[1], Chunhua Jian[1], Chen Wang[1], Wei Li[1], Yunting Xie[1], Chunbao Li[1], Changbo Tang[2], Shijie Ding[1*], Liang Zhao[2,3*], Guanghong Zhou[2*]

[1]Joes Future Food Technology Co. Ltd, Nanjing 211225, Jiangsu, PR China

[2]State Key Laboratory of Meat Quality Control and Cultured Meat Development, College of Food Science and Technology, Nanjing Agricultural University, Nanjing 210095, Jiangsu, PR China

[3]College of Animal Science and Technology, Nanjing Agricultural University, Nanjing 210095, China

[4]These authors contributed equally: Huifang Li, Haozhe Zhu, Zhongyuan Wu

* Corresponding authors, E-mail:

dingshijie@joesfuturefood.com

liang.zhao@njau.edu.cn

guanghong.zhou@hotmail.com

Abstract

Cell lines suitable for serum-free suspension culture remain limited for cultured meat production. Here, we established a spontaneously immortalized porcine muscle-derived cell line by adapting a satellite-cell-enriched primary culture to serum-free suspension without genetic modification. Cells completed more than 255 population doublings by day 300. Longitudinal single-cell transcriptomics revealed shifts from myogenic to mesenchymal stromal-like and then adipogenic-like states during adaptation. The cells showed little basal lipid accumulation but inducible adipogenesis, with no detectable myogenic differentiation. They retained DNA damage recovery capacity and exhibited no detectable tumorigenicity. Compared to fed-batch or cell-retention perfusion culture, semi-continuous culture improved medium-use efficiency, requiring less dry medium per unit of wet biomass. Scale-up in a 2,000-litre bioreactor yielded 97.18 kg wet biomass with a medium conversion ratio of 0.63:1 (dry medium/wet biomass). These results provide a porcine cell source and a semi-continuous process for scalable production of cultured pork biomass.

Key words: cultured meat; porcine cells; serum-free suspension culture; cell state transition; scale-up production

Introduction

Meeting the growing global meat demand through conventional livestock production is challenging because of its environmental impacts, resource requirements and animal welfare concerns.[1-4] Cultured meat, produced by expanding animal cells into edible biomass and/or tissues, has therefore emerged as a potential complement.[5, 6] Realizing this potential at commercially relevant scales depends on resolving persistent bottlenecks in production cell-line development, serum-free medium design, bioprocess engineering, etc.[6, 7]

Primary cells, including muscle stem cells, fibro-adipogenic progenitors, adipose-derived stem cells, and fibroblasts, are potential cell sources.[8-10] However, their proliferative capacity and differentiation potential decline during extended passaging.[11] Pluripotent stem cells have greater self-renewal and multilineage potential, but require complex species-specific culture and differentiation protocols.[6] Immortalization of primary cells has been achieved by targeting the cell-cycle inhibitors p15 and p16, or by introducing TERT with CDK4. Such genetic modification requires careful assessment of genomic stability and cellular properties and may also raise regulatory considerations.[12-14] Spontaneous immortalization could provide a non-transgenic alternative. Such cell lines have been reported in avian, bovine, and porcine cells.[13, 15-17] However, in porcine muscle-derived cells, spontaneous immortalization during serum-free suspension adaptation and the accompanying changes in cell states remain poorly understood.

For large-scale production, a suitable cell source must also support serum-free culture and efficient expansion. Eliminating animal serum reduces dependence on a costly and variable component.[7, 18] Serum-free media have supported the sustained

expansion of bovine satellite cells.[19, 20] Fed-batch, cell-retention perfusion and continuous culture strategies differ in nutrient supply, metabolite removal and biomass recovery, making biomass yield and medium consumption important considerations for process development.[21, 22] Perfusion culture has enabled repeated harvesting of chicken biomass in animal-free medium.[19] Scale-up introduces additional constraints, including metabolite accumulation and limitations in oxygen transfer and mixing, that can impair cell growth and biomass productivity.

Here, we obtained a spontaneously immortalized porcine muscle-derived cell line by adapting a satellite-cell-enriched primary culture to serum-free suspension without genetic modification. Single-cell transcriptomics across nine stages showed that the adapted cells gradually acquired adipogenic features during long-term culture. After replating under adherent conditions, the cells could differentiate into adipocytes, whereas myogenic differentiation was not detected. We assessed safety-related cellular properties and compared fed-batch, cell-retention perfusion, and semi-continuous culture for biomass production. The semi-continuous culture was further tested in a 2,000-litre bioreactor. We quantified biomass output and medium consumption, examined the effect of medium price on medium cost per kilogram of biomass, and incorporated the harvested biomass into a hybrid food product. Together, these results establish a cell source and an experimentally evaluated process for scalable production of cultured pork biomass.

Results

Spontaneous immortalization during serum-free suspension adaptation

We expanded our primary porcine skeletal muscle satellite cell-enriched population in adherent monolayers (P1-P8) and on porous microcarriers (P9; Fig. 1a, b). Cells were

then transferred to serum-free medium under orbital agitation, and initially formed aggregates progressively dispersed into a single-cell suspension by day 141 (SD141; Fig. 1b). Two major proliferative bottlenecks were observed during adaptation. The population-doubling time (PDT) increased from 26.9 h before adaptation to 192.4 h at SD6 and peaked at 603.1 h at SD56 (Fig. 1c, d). Proliferation subsequently recovered, with cumulative population doublings exceeding 102 by SD141, surpassing the operational threshold of 100 cumulative PDs used to define immortalization, and 255 by SD300, calculated from P0 (Fig. 1e). The PDT decreased to 23.4 h by SD175 and thereafter remained between 18 and 26 h, without subsequent proliferative decline (Fig. 1c, d). This process did not involve genetic modification. Therefore, cells after SD300 were designated as a spontaneously immortalized porcine muscle-derived cell line.

To characterize the molecular features of the SD300 line, we compared TERT and transcripts related to TP53 signalling and cell-cycle regulation between P5 and SD300 cells. *TERT* expression was 2.6-fold higher in SD300 cells (Fig. 1f), while telomerase activity was maintained (Extended Data Fig. 1). *TP53* expression was also increased, whereas *TP53RK* and *TP53I3* showed no differences ($P > 0.05$). Among the cell-cycle-related genes examined, *CDK4* expression was higher, whereas *CCNB1*, *CCND1*, and *CDK1* expression was lower in SD300 cells (Fig. 1f).

Cell-state remodelling during suspension adaptation

We conducted a systematic scRNA-seq analysis to resolve cell-state remodelling during suspension adaptation. Four transcriptional states, myogenic (Myo), mesenchymal stromal-like (Mes), extracellular matrix-remodelling (ECM-R), and adipogenic-like (Adip), were identified (Fig. 2a,b,c; Extended Data Fig. 2a). The Myo

fraction decreased from 98% at P5 to 17% at P7, whereas Mes cells accounted for 88% at P9. ECM-R cells predominated at SD7 (86%) but declined to 55% at SD17. Adip cells increased from 13% at SD7 to 99% at SD38 and remained dominant through SD300 (Fig. 2c and Extended Data Fig. 2b). This state was enriched for lipid-metabolic processes (Extended Data Fig. 2a).

Pseudotime analysis placed Mes between the loss of the Myo programme and the emergence of the Adip-associated programme (Extended Data Fig. 3a). Among surviving cells at SD7 and SD17, pseudotime and RNA velocity suggested divergence from an Adip-associated region towards ECM-R or within Adip (Fig. 2d,e and Extended Data Fig. 3b). By SD38, trajectories were largely confined to Adip. The ECM-R-associated path showed matrix-remodelling, stress- and apoptosis-related programmes (Extended Data Fig. 4a). Along the Adip-retaining path, cell-cycle-associated Module 2 expression peaked near the root, preceding increased lipid-metabolic Module 1 expression (Fig. 2f,g and Extended Data Fig. 4b,c).

Culture from SD38 to SD300 involved nutrient enrichment followed by transfer to a food-compatible medium. Cell cycle scoring showed that the G1 fraction declined from 93% at SD17 to 5% at SD300, whereas G2/M increased from 3% to 74% (Extended Data Fig. 5c). Temporal clustering of the 100 most variable genes identified declining signalling, adhesion, stress-response, and matrix-remodelling programmes, alongside increasing lipid-metabolic gene expression, including *LPL*, *FASN*, *FABP4* and *ADIPOQ* (Extended Data Fig. 5d-h). These genes showed broadly similar expression patterns at SD277 and SD300, before and after transfer to food-compatible medium, respectively.

SD300 cells lose myogenic ability but acquire inducible adipogenic potential

The stable Adip-like state and elevated lipid-metabolic features suggested an altered lineage of adapted cells. Compared to the parental P5 cells, PAX7 staining was nearly undetectable, vimentin staining was reduced, and PDGFRA staining was increased in SD300 cells after replating under adherent conditions (Fig. 3a). Expression of *PAX7*, *MYF5*, *MYOD1*, and *MYOG* was also dramatically lower (Fig. 3b). Consistently, scRNA-seq showed lower *PAX7* and *ITGB1* but higher *PDGFRA* and *VCAM1* expression in Adip than in Myo cells (Extended Data Fig. 6a,b). After myogenic induction, P5 cells formed MyHC-positive multinucleated myotubes, whereas SD300 cells showed no detectable myotube formation and a near-zero differentiation index (Fig. 3c). Induced SD300 cells also showed lower *MYOD1* and nearly undetectable *MYOG* expression than P5 cells (Fig. 3d).

Under non-inducing conditions, SD300 cells showed modest lipid accumulation despite higher basal *CEBPA*, *PPARγ*, and *FABP4* expression than P5 cells (Fig. 3e and Extended Data Fig. 6c). Following adipogenic induction, SD300 cells accumulated abundant lipid droplets, whereas P5 cells responded weakly (Fig. 3f). *PPARγ* and *FABP4* expression was also higher in induced SD300 cells than in induced P5 cells (Fig. 3g).

We next compared SD300 transcriptomes with those of porcine tissues and primary cell cultures. Principal component analysis (PCA) positioned SD300 cells near subcutaneous and visceral adipose tissues, separate from skeletal muscle and liver (Fig. 3h). However, heatmap analysis showed distinct gene-expression patterns between SD300 cells and both adipose tissues (Extended Data Fig. 6d). Further comparisons with satellite cells and intramuscular and subcutaneous preadipocytes before and after differentiation revealed a distinct profile from these primary cells (Fig. 3i). The gene expression pattern of SD300 more closely resembled that of

parental P5 cells (Fig. 3j). Together, these findings supported an adipogenic-primed state with inducible adipogenic potential but no detectable myogenic competence.

Authentication and safety characterization of the SD300 cell line

We confirmed the species origin of the SD300 cell line and determined the microbiological condition and safety characteristics. The PCR products of mitochondrial D-loop and cytochrome b amplicons from porcine but not from chicken were detected in SD300 cells (Fig. 4a). Independent third-party testing found no bacterial, fungal, mycobacterial or Mycoplasma contamination and no evidence of the adventitious agents included in the testing panel (Extended Data Table 1). Additional testing for porcine viruses, including African swine fever virus (ASFV), classical swine fever virus (CSFV) and foot-and-mouth disease virus (FMDV), was also negative (Fig. 4b and Extended Data Table 1). SD300 cells also expressed lower levels of selected prion- and amyloid-related genes, including *PRNP*, *APP*, *PSEN1*, and *BACE1* compared to P5 cells (Fig. 4c).

We measured DNA damage kinetics by quantifying nuclear γH2AX foci. Their quantity increased in both P5 and SD300 cells following DNA-damaging treatment and decreased after recovery, with no differences from untreated controls (Fig. 4d,e).

Finally, potential tumorigenicity was evaluated using complementary *in vitro* and *in vivo* assays. HeLa cells formed readily detectable colonies after 21 days in soft agar. In contrast, neither P5 nor SD300 cells formed colonies (Fig. 4f). Consistently, mice injected with SD300 cells showed no evidence of tumor formation during the observation period, while obvious tumors developed in the positive-control group (Fig. 4g). Histological examination of brain, heart, liver, lung, spleen, and kidney sections

revealed no detectable metastatic lesions in either the SD300 or positive-control group (Extended Data Fig. 7a-f).

These findings support the microbiological quality and non-tumorigenic phenotype of SD300 cells and provide an initial safety-related characterization for their further development as a production cell line for cultured pork.

Semi-continuous culture supports sustained biomass production

Using the stable and food-compatible immortalized SD300 cell line, we next compared three serum-free production configurations in 50-litre bioreactors to select a process for further scale-up (Fig. 5a-g). Fed-batch culture reached a maximum viable cell density of 103.70×10^5 cells ml^{-1} on day 5, then declined in density and viability as ammonium built up (Fig. 5a,b). The process generated 935.13 g of accumulated biomass using 33.85 litres of medium in total, equivalent to 900.02 g of dry medium. This corresponded to a dry-medium-to-wet-biomass ratio of 0.96 kg kg^{-1}, defined here as the medium conversion ratio (Fig. 5g).

Cell-retention perfusion in rocking-motion bioreactors reached 562.67×10^5 cells ml^{-1} on day 12 while maintaining high viability (Fig. 5c,d). Medium exchange limited the progressive accumulation of lactate and ammonium during the monitoring period, although glucose was nearly depleted late in culture (Fig. 5d). The process produced 1028.15 g of wet biomass using 256.37 litres of medium, corresponding to 3640.38 g of dry medium with a medium conversion ratio of 3.54 (Fig. 5g).

Semi-continuous culture in stirred-tank bioreactors maintained high viability and provided ten consecutive 24-h harvests with a target harvest density of 6.0×10^6 viable cells ml^{-1} during a 13-d run, without progressive lactate or ammonium accumulation (Fig. 5e,f). The process generated 6585.30 g of wet cell biomass using

287.18 litres of medium, equivalent to 5077.40 g of dry medium and a medium conversion ratio of 0.77, the lowest among the three processes examined (Fig. 5g). Consequently, semi-continuous culture showed the lowest dry medium requirement per unit biomass, the highest cumulative biomass output, and sustained harvesting among the three configurations, even though perfusion achieved the highest cell density.

Scale-up of semi-continuous culture in a 2,000-litre bioreactor and cost analysis

For scale-up, SD300 cells were further adapted to serum-free production medium DP19421812 and banked as JF108-SWCB-FB2. Starting with 40×10^6 cells, cells were expanded through 125-ml and 1-litre shake flasks and 3-, 20–50-, 50- and 200-litre bioreactors before transfer to the 2,000-litre production vessel (Fig. 6a). The seed train generated 2.15×10^{12} cells while maintaining viability above 90%, with a mean doubling time of 20.68 ± 3.86 h (Extended Data Fig. 8a,b).

The production vessel was inoculated with 1.75×10^{12} viable cells at an initial density of 19.9×10^5 cells ml^{-1}, corresponding to an initial working volume of approximately 880 litres. Semi-continuous culture continued for 6 d, with collections on days 18, 20 and 22 (Fig. 6b, c). Cumulative wet biomass reached 97.18 kg by day 22 (Fig. 6d). Glucose remained available and lactate low, whereas ammonium reached approximately 14 mM by day 22 (Extended Data Fig. 8c). Cells retained a predominantly round morphology at the sampled stages (Extended Data Fig. 8d). Protein and fat contents were comparable across the three harvests, averaging 59.56 g and 10.24 g per 100 g of dry biomass, respectively (Fig. 6e).

The complete process consumed 2,925 litres of medium (61.02 kg dry medium), corresponding to a cumulative wet biomass yield of 3.32% (w/v) and a medium

conversion ratio of 0.63 kg kg^{-1} (Fig. 6c, Extended Data Fig. 8e). Medium nutrients and single-use consumables dominated the estimated cost of goods (Fig. 6f). At the current medium price of US$9.41 l^{-1}, medium use contributed US$283.23 per kilogram of wet biomass. At a reduced medium price of US$0.63 l^{-1}, as projected for a 50,000-litre production facility, the medium cost contribution would decrease to US$18.96 kg^{-1}, assuming unchanged medium consumption and biomass output.

The collected biomass was then mixed with high-moisture extruded soy protein and formed into a hybrid spring roll, demonstrating its compatibility with downstream food processing (Fig. 6g). Electronic-nose PCA placed the 47% biomass formulation closer to the positive control than the 20% formulation (Fig. 6h). Electronic-tongue responses showed that the responses of bitter and astringent aftertaste were lower (47%) and the responses of richness, umami, and saltiness were higher than the negative control (Fig. 6i).

Discussion

Serum-free suspension production has been demonstrated with spontaneously immortalized chicken fibroblasts,[13] whereas porcine FaTTy cells were expanded in serum-containing adherent culture,[16] and spontaneously immortalized porcine myoblasts and fibroblasts were maintained in suspension with 1% serum.[23] Our previous studies achieved prolonged serum-free expansion of porcine myogenic cells through CDKN2A disruption or TERT/CDK4 co-expression, while retaining myogenic potential.[24, 25] Here, spontaneous immortalization during serum-free suspension adaptation yielded an adipogenic-primed line that showed inducible adipogenesis but no detectable myogenesis and supported semi-continuous culture in a 2,000-litre production vessel.

The major change in cell state shifts occurred early in adaptation. Myogenic features declined during adherent expansion, and Adip predominated by SD38 following extensive cell death during early suspension adaptation. Similar compositional changes were also reported in bovine satellite-cell cultures, where FAP abundance increased from 1% to 93.6% over six passages.[26-29] Adipogenic differentiation of sorted porcine $CD45^{-}$ $CD56^{+}$ myogenic cells,[30] and our previous inference of density-dependent FAP-like transitions also raise the possibility of phenotypic plasticity.[31] Selection and plasticity may therefore both contribute to Adip predominance, although lineage tracing is needed to distinguish their contributions.[32]

The lipid metabolic characteristic continued to strengthen from SD38 to SD300 during spontaneous immortalization and sustained proliferation. Suspension adaptation of DF-1 chicken fibroblasts was also accompanied by changes in PPAR signalling and increased adipogenic potential.[33] Studies in other cell systems link lipid metabolism to redox control and survival after loss of matrix attachment.[34, 35] Whether these pathways support survival or proliferation in the present line remains to be determined.

Despite their proximity to adipose tissues in principal-component space, SD300 cells accumulated little lipid without induction. They were transcriptionally distinct from parental P5 cells and primary myogenic and adipogenic reference populations. This phenotype could allow separate optimization of biomass expansion and lipid accumulation, as proposed for other adipogenic cell systems.[29, 36, 37] However, the loss of myogenesis limits their direct use for muscle-tissue formation. Incorporation of the harvested biomass into a hybrid food prototype is consistent with previous use of cultured adipocyte-like cells in soy-based products.[13]

Production data for immortalized cells remain limited in cultured meat. Fed-batch operation is relatively simple but does not continuously remove metabolites, which can limit culture duration and requires culture restart for subsequent production cycles. Perfusion enables medium exchange and higher cell densities but requires additional cell-retention equipment and may increase medium consumption.[38] Immortalized chicken fibroblasts reached 108×10^6 cells ml^{-1} in serum-free perfusion culture.[13] More recently, perfusion in animal-component-free medium supported 12 harvests over 20 days, yielding 1.7 kg of wet biomass at a working volume of 1.8 litres.[21] In our comparison, cell-retention perfusion achieved the highest cell density but consumed more medium per unit biomass. Semi-continuous culture allowed repeated harvesting without restarting the culture, reducing the need for repeated seed preparation and associated consumables. Although it achieved a lower cell density than perfusion, semi-continuous culture produced the highest cumulative biomass output with the lowest dry medium consumption per kilogram of wet biomass. Its subsequent scale-up in a 2,000-litre vessel yielded 97.18 kg of wet biomass with a medium conversion ratio (MCR) of 0.63:1 (dry medium/wet biomass). This ratio was numerically lower than the feed conversion ratio (FCR) of approximately 2-3 kg feed per kg live-weight gain reported for growing-finishing pigs, although differences in input materials and biomass composition preclude direct comparison.[39] The low ratio nevertheless indicates the potential for efficient conversion of medium nutrients into cultured meat biomass.

Medium price remained a major constraint for cultured meat production.[19, 21] At US$9.41 l^{-1}, medium contributed US$283.23 per kilogram of wet biomass. The projected contribution of US$18.96 kg^{-1} assumes a medium price of US$0.63 l^{-1}, as reported for cultured chicken,[21] with unchanged biomass output and medium

consumption. The wet biomass yield in our 2,000-litre semi-continuous production run was 3.32% (w/v), compared with 36% (w/v) reported for immortalized chicken fibroblasts in perfusion culture.[13] Although the cultivation strategies differ, this comparison suggests room for improving biomass yield. Doubling biomass yield without increasing medium consumption would further reduce the medium cost to US$9.48 kg^{-1}. Recently, PARIMA reported multi-tonne cultivated duck production using Vow's 22,000-litre bioreactor, with a stated production cost target below €10 kg^{-1}. Although this target cannot be directly compared with our medium-only estimate, it illustrates the progress towards lower-cost production at larger scales.

The cellular origin of the adapted state and its stability across independent cultures remain to be established. Lineage tracing and genomic characterization, together with independent adaptation and production runs, would help establish how reproducibly this phenotype can be obtained and maintained. This study provides a porcine cell source and measured process requirements for serum-free suspension production of cultured pork biomass.

Methods

Materials

DMEM/F12 (C11330500BT), foetal bovine serum (10091-148), penicillin-streptomycin solution (15140-22), ITS-X (51500056), Anti-Clumping Agent (0010057AE), TrypLE Express enzyme (12604054), lipid supplement (11905031), NEAA (11140050), yeast extract (212750), BCA assay kit (A55860) and Phusion Plus DNA polymerase (F630) were purchased from Thermo Fisher Scientific. Collagen I, rat tail, 0.05% (254236) was purchased from Corning. Microcarriers (P0-100) and digestion reagent (R001-500) were purchased from CytoNiche. Bovine

HGF (Z03803), bFGF (Z03230-5), IGF-1 (Z03688), LIF (Z03802) and porcine EGF (Z03777-1) were purchased from GenScript. Zinc sulfate heptahydrate (Z0251), vitamin C (A5960), vitamin E (258024), and sodium selenite (S9133) were obtained from Sigma-Aldrich. Cortisol (M3451) was purchased from AbMole, and CD02C medium (A11002) was purchased from QuaCell. The RNA Isolation Kit (RC101-01), HiScript III RT SuperMix (+gDNA wiper; R323-01), and SYBR Master Mix for qPCR (Q311-02) were obtained from Vazyme. The DNA extraction kit (9765) was purchased from Takara Bio. Etoposide (12092) was purchased from Wuhan Aimeijie, and GelGreen (D0143) was purchased from Beyotime.

Primary cell isolation and 2D adherent culture

Porcine muscle-derived primary cells were isolated from skeletal muscle of 1-week-old pigs as we previously reported.[40] $CD31^{-}CD45^{-}CD56^{+}CD29^{+}$ cells were enriched by fluorescence-activated cell sorting. After isolation, cells were maintained on collagen I-coated dishes in F10 medium supplemented with 20% FBS, 5 ng ml^{-1} bFGF, and 1% penicillin–streptomycin. Cells were passaged every 3 days and transferred to microcarrier culture at P9.

3D microcarrier-based adherent culture

At P9, cells were transferred into a bioreactor containing DMEM/F12 supplemented with 1-5 mg ml^{-1} microcarrier tablets and 15-20% fetal bovine serum.[41] Half of the culture medium was replaced with fresh medium after 2-4 days. After 6-7 days, half of the medium was removed, and microcarrier dissolution reagent was added to a final concentration of 1-2 mg ml^{-1}. Following complete microcarrier dissolution, cells were

harvested by centrifugation and cryopreserved as seed cells for subsequent suspension adaptation.

Serum-free suspension adaptation and step-wise medium optimization

Cryopreserved microcarrier-cultured cells were thawed and inoculated into 125-ml shake flasks at 0.5×10^6 cells ml^{-1}. Cells were initially cultured in serum-free medium-1 (SFM-1), comprising A24 serum-free medium[25] supplemented with forskolin, anti-clumping agent and Pluronic F-68 from SD0 to SD7. To promote suspension adaptation, AM-2395 and yeast extract were added to SFM-1 to prepare SFM-2, which was used after SD7. From SD38 to SD277, the A24 basal medium in SFM-2 was replaced with CD02C medium (SFM-3), to provide enhanced nutrient support for spontaneous immortalization and long-term proliferation. From SD277 to SD300, SFM-3 was reformulated without Y-27632·2HCl, AM-2394, dexamethasone, Trolox or N-acetylcysteine (SFM-4) to reduce the potential carryover of medium additives into the harvested biomass and improve its suitability for food production.[42, 43] The SD300 cells were banked as S-WCB for relevant testing.

Flasks were agitated at 90 rpm initially and at 120 rpm after SD18. Cell aggregates gradually decreased in size, and the culture was predominantly a single-cell suspension by approximately SD141. Cell growth, viability and metabolite concentrations were monitored throughout adaptation. Cells were maintained in serum-free suspension culture through SD300 before establishment of the working cell bank.

382

383 **Single-cell RNA sequencing and analysis**

384 Cells collected for scRNA-seq included adherent cells at P7, microcarrier-cultured
385 cells at P9, and cells collected after 7, 17, 38, 147, 277 and 300 days of suspension
386 adaptation. P5 data were obtained from our previous study using the same
387 library-preparation workflow.[31] Single-cell suspensions were assessed for viability
388 and concentration before loading onto a Chromium Controller. cDNA libraries were
389 constructed using the Chromium Single Cell 3' Library & Gel Bead Kit v3 according
390 to the manufacturer's instructions (10x Genomics). Libraries were sequenced on an
391 Illumina NovaSeq 6000 S4. Reads were processed using cellranger (v.9.0.0) against
392 Sus_scrofa 11.1.

393 Datasets from the nine samples were integrated and analysed in R using Seurat
394 (v.5.3.0).[44] After quality control, 108,960 cells and 17,093 features were retained,
395 with median values of 3,712 detected genes and 12,403 unique molecular identifier
396 (UMI) counts per cell. Data were normalized and scaled using SCTransform (v.0.4.2),
397 and batch effects among samples were corrected using Harmony (v.2.0.5). Cell-cycle
398 phases were assigned using the cell-cycle scoring functions implemented in Seurat.
399 Differential gene expression was analysed using the FindMarkers function with the
400 Wilcoxon rank-sum test, and genes with Bonferroni-adjusted $P < 0.05$ were
401 considered differentially expressed.

402 UMAP embedding generated in Seurat was implemented in Monocle 3 for
403 pseudotime trajectory analysis. Loom files with spliced and unspliced transcript

counts were used for RNA velocity analysis using scVelo (v.0.3.4) in Python, and velocity streamlines were also projected onto the UMAP embedding. Gene Ontology (GO) enrichment analysis and gene set enrichment analysis (GSEA) were performed using clusterProfiler v.4.12.6. Terms with nominal $P < 0.05$ and false discovery rate-adjusted $q < 0.05$ were considered significantly enriched.

Bulk RNA sequencing and analysis

Bulk RNA-seq data generated from P5 and SD300 cells were analysed together with publicly available porcine RNA-seq datasets. Raw reads from all datasets were processed using the same pipeline. Reads were filtered using SOAPnuke (v.2.2.1) and aligned to the porcine reference genome using HISAT2 (v.2.2.1). Clean reads were also mapped to the reference gene set using Bowtie2 (v.2.4.5), and gene expression was quantified using RSEM (v.1.3.1) as fragments per kilobase of transcript per million mapped reads (FPKM). PCA was performed in R using the princomp function after centring and scaling the FPKM expression matrix. Heatmaps were generated from the FPKM expression matrix using pheatmap (v.1.0.12).

Two comparisons were performed. First, SD300 cells were compared with reference datasets from liver,[45] skeletal muscle,[46] visceral adipose tissue,[47] and subcutaneous adipose tissue.[47] Second, SD300 cells were compared with P5 cells and publicly available datasets representing primary satellite cells,[48] myogenically differentiated satellite cells,[49] and subcutaneous fat-derived and intramuscular fat-derived adipogenic cells before and at days 4 and 8 of adipogenic differentiation.[50]

Three biological replicates were included for each cell type or condition. Accession numbers and sample details are provided in Supplementary Table 1.

Myogenic and adipogenic induction

For myogenic induction, P5 and SD300 cells (1×10^5 cells per dish) were seeded onto Matrigel-coated dishes. After reaching 90% confluence, the proliferation medium was replaced with serum-free myogenic differentiation medium (JFMYOINS3, Joes Future, Nanjing), which was refreshed every 2 days. Cells were collected after 6 days of induction.[24]

For adipogenic induction, P5 and SD300 cells were seeded separately onto collagen-coated dishes at 0.1×10^6 cells per dish. At approximately 90% confluence, proliferation medium was replaced with serum-free adipogenic induction medium 1 (Joes Future Food; JFAPC3-1). Medium 1 was renewed every 2 days during the first 5 days. On day 5, cells were transferred to 2 ml of medium 2 (JFAPC3-2) per dish. On day 7, this was replaced with 2 ml of medium 3 (JFAPC3-3). Medium 3 was renewed on day 9, and differentiation ended on day 10.[51]

Quantitative RT-PCR

The FastPure Cell/Tissue Total RNA Isolation Kit (Vazyme, RC101-01) was used for total RNA extraction. Subsequently, cDNA was reverse-transcribed with HiScript III RT SuperMix for qPCR. qRT-PCR was performed on a BIO-RAD CFX Opus 96

real-time PCR system using ChamQ SYBR qPCR Master Mix . Primer sequences are listed in the Supplementary Table 2.

Telomerase activity assay

The telomeric repeat amplification protocol (TRAP) was followed.[52, 53] Cells were washed with cold PBS and lysed in 500 μl CHAPS-based lysis buffer for 30 min. Lysates were centrifuged at 13,000 × g for 40 min at 4 °C, and protein concentrations were determined using a BCA assay kit. For each reaction, 5 μg protein was used for TRAP amplification with TS, ACX, NT and TSNT primers (Supplementary Table 2). PCR products were separated on 12% non-denaturing polyacrylamide gels, stained with GelGreen and imaged using a UVP imaging system.

Immunofluorescence staining

Cells were fixed with 4% paraformaldehyde for 15-30 min, permeabilized with 0.5% Triton X-100 for 15 min and blocked with 5% BSA or goat serum. Primary antibodies include PAX7 (AB528428, DSHB), vimentin (ab8978, Abcam), PDGFRA (ab203491, Abcam), and γH2AX (9718T, Cell Signaling Technology). Appropriate Alexa Fluor-conjugated secondary antibodies (A11034 and A11029, Thermo Fisher Scientific) was used. Nuclei were counterstained with DAPI. Fluorescence images were acquired using a confocal microscope (DMi8, Leica).

Species identification

Genomic DNA was isolated from SD300 cells using the Takara DNA extraction kit following manufacturer's instructions. Species-specific PCR was performed in a 50-μL system with 100 ng template DNA using Phusion Plus DNA polymerase. 18S rRNA was used as internal control. Primer sequences are provided in the Supplementary Table 2.

DNA-damage induction and recovery

P5 and SD300 cells were seeded on collagen-coated glass-bottom dishes at 1×10^4 cells per well. After 48 h, cells were treated with 2.5 μM etoposide for 2 h and collected immediately or after 10 h of recovery in fresh medium without etoposide. Untreated cells served as controls. For immunofluorescence staining, cells were fixed with 4% paraformaldehyde, permeabilized with 0.5% Triton X-100 and blocked with 5% BSA. Cells were incubated with an antibody against γH2AX (9718T, Cell Signaling Technology), followed by an Alexa Fluor-conjugated anti-rabbit secondary antibody. Nuclei were counterstained with DAPI. γH2AX foci were imaged by confocal microscopy (DMi8, Leica).[54]

Soft agar colony formation assay

For the soft agar colony formation assay, a bottom layer containing 0.5% agar in culture medium was added to 6-well plates (1.5 ml per well) and allowed to solidify for 30 min. SD300 cells were seeded at 1.2×10^4 cells per well in 0.3% agar as a 1.5-ml top layer, with HeLa cells (CL-0001, Wuhan Pricella Biotechnology Co., Ltd.)

included as the positive control. A cell-free preparation instead of the cell suspension was used as the negative control. After solidification, 100 µl culture medium was added to each well and replaced twice weekly. Cells were cultured for 21 days, and colony formation was monitored by microscopy. On day 21, colonies were stained with 200 µl Nitro Blue Tetrazolium (NBT) solution overnight at 37 °C and photographed.

In vivo tumorigenicity and histological examination

In vivo tumorigenicity was assessed by an independent testing laboratory (Wuhan Canvest Biotechnology Co., Ltd.). SD300 cells (1×10^7 viable cells per mouse) were inoculated into ten nude mice and monitored for up to 125 days. The 2BS cell line and H22 cells were included as negative and positive controls, respectively, with ten mice per group. One mouse in the SD300 group died during the observation period. At the end of the study, major organs were collected and examined histologically for tumour formation. Histopathological examination was performed on major organs.

Fed-batch, cell-retention perfusion and semi-continuous culture

SD300 cells from the working cell bank were expanded in serum-free medium in shake flasks at an initial density of $2 \pm 0.5 \times 10^5$ cells ml^{-1}. Detailed culture parameters and process data for the three bioreactor configurations are provided in Supplementary Table 3. Fed-batch and semi-continuous cultures were performed in 50-litre stirred-tank bioreactors, whereas cell-retention perfusion used 50-litre

rocking-motion bioreactors. Cultures were maintained at 37 ± 0.5 °C, pH 7.2 ± 0.2, CO_2 at 5 ± 1 % and dissolved oxygen at 40 ± 2 %. Stirred-tank agitation was set to 120 ±10 rpm, and the rocking angle was 7 ± 1°, 20-25 rpm. Three independent production runs were performed for each configuration.

For fed-batch culture, the feed media consisted of QuaCell® CHO Feed02 Supplement and SFM-4 factor kit. Both feeds were supplemented at 5% of the culture working volume on day 3, followed by identical feeding every two days until the end of culture.. For cell-retention perfusion, spent medium was continuously removed through a cell-retention membrane integrated into the single-use WAVE cellbag and replaced with fresh medium, while cells were retained in the vessel. Perfusion was initiated on day 3 at 0.5 vessel volumes per day (VVD) and increased to 2 VVD from day 5. VVD was defined as the daily medium-exchange volume divided by the culture working volume. For semi-continuous culture, harvesting was initiated on day 3 when the viable cell density reached approximately 6×10^6 cells ml^{-1}.Cell-containing culture was withdrawn and replaced with an equal volume of fresh medium to maintain the working volume. Ten harvests were collected during the 13-day run.

Viable cell density and viability were measured using an automated cell counter (Countstar Mira FL, Shanghai Ruiyu Biotechnology, China). Cell suspensions were mixed with trypan blue and loaded into counting chambers for automated enumeration of live and dead cells. Culture samples were centrifuged to remove cells before metabolite analysis. Glucose, lactate and ammonia concentrations in the supernatants were measured using an automated biochemical analyser (AU200,

Beijing Aipscience Biotechnology, China). Measurements used commercial assay kits according to the manufacturers' instructions.

Seed-train expansion and production in a 2,000-litre bioreactor

SD300 cells were subsequently adapted to serum-free medium DP19421812 (Joes Futurefood, Nanjing), formulated to reduce medium cost and growth-factor use while addressing potential safety concerns. The adapted cells were banked as JF108-SWCB-FB2. Seed-train expansion began with two JF108-SWCB-FB2 cryovials containing 40×10^6 cells. Cells were expanded in 125-ml and 1-litre shake flasks, a 3-litre stirred-tank bioreactor, a 20–50-litre Wave bioreactor, and 50- and 200-litre stirred-tank bioreactors before transfer to the 2,000-litre production vessel. Serum-free conditions were maintained throughout expansion and production.The production vessel was inoculated with 1.75×10^{12} viable cells at an initial density of 1.99×10^6 cells ml^{-1} and an initial working volume of approximately 880 litres. Three harvests were collected on process days 18, 20 and 22. Process day 0 was defined as the start of seed-train expansion. Cell density, viability, and glucose, lactate, and ammonia concentrations were monitored throughout cultivation using the methods described above.

Harvested cell suspensions were transferred to an Alfa Laval MB20 disc-stack centrifuge operated at 3,500 rpm and concentrated to 10% of their original volume. Four volumes of washing solution (JFWASH-Y, Joes Futurefood, Nanjing) were then added, and the suspension was reconcentrated to 20% of the combined volume. This

557 washing and concentration procedure was repeated four times. The recovered biomass
558 was weighed, and cumulative wet biomass was calculated as the sum of biomass from
559 the three harvests.
560
561 **Medium consumption and cost analysis**
562 Accumulated medium volume was recorded across the entire run for each process
563 configuration, and the corresponding medium dry weight was calculated from the
564 formulated powder mass used to prepare the medium. Accumulated biomass was
565 determined by harvesting and weighing the cell slurry. The medium conversion ratio
566 was calculated as the dry medium consumed divided by the wet biomass harvested (g
567 g^{-1}). Medium cost per kilogram of wet biomass was calculated from the total medium
568 volume consumed, medium price, and biomass output. For the 2,000-litre production
569 run, medium costs were calculated using the current medium price of US$9.41 l^{-1} and
570 a reduced-price scenario of US$0.63 l^{-1} reported for a 50,000-liter production
571 facility,[21] assuming unchanged medium consumption and biomass output.
572
573 **Hybrid food product preparation**
574 Four spring-roll formulations were prepared: a negative control in which cell biomass
575 was replaced with 225g water, a positive control containing 225 g of conventional
576 pork (17.5 g protein and 3 g fat), and two experimental groups containing 95.74 g
577 (20%, w/w) or 225 g (47%, w/w; 17.5 g protein and 3 g fat) of cell biomass relative to
578 the total spring-roll weight. Each formulation contained 75 g of textured soy protein.

Fresh shepherd's purse was washed, blanched, cooled, drained and chopped. Textured soy protein and the corresponding amount of pork, cell biomass or water were stir-fried. Chopped shepherd's purse (80 g) was then added, followed by minced ginger, scallions, salt, vegetable oil and egg. The filling was mixed, wrapped in spring-roll wrappers, sealed with a flour-based slurry and shaped. The spring rolls were deep-fried at 160-170 °C for 4-5 min and drained before analysis.

Electronic-nose and electronic-tongue analyses

Volatile profiles were analysed using a PEN3 electronic nose (Airsense Analytics, Schwerin, Germany). About 3 g samples were placed in 20-ml headspace vials and sealed. The vials were incubated at 37 °C for 30 min and then equilibrated at 25 °C for 30 min. Headspace gas was introduced into the sensor chamber through a needle, with a second needle used to maintain pressure. The instrument was set as previously reported.[55] Taste profiles were analysed using an SA402B electronic tongue (Insent Intelligent Sensor Technology Inc., Kanagawa, Japan). About 30 g samples were mixed with 200 ml ultrapure water at 40 °C, homogenized at 5,000 rpm for 2 min and centrifuged at 10,000 × g for 20 min. The supernatant was filtered through three layers of medical gauze before analysis. The five sensors were activated and calibrated before measurement. Three independent replicates were analysed, with two parallel measurements for each replicate. Sensor characteristics for both analysis are provided in Supplementary Table 4.

Statistical analysis

Cell culture experiments were performed in three independent batches. Bulk RNA-seq included three biological replicates per group. Each production configuration was tested in three independent runs. Two-group comparisons were performed using two-tailed t-tests. Comparisons among more than two groups were performed using one-way ANOVA followed by Tukey's multiple-comparisons test. Data are presented as mean ± SD. $P < 0.05$ was considered statistically significant.

Data availability

Single-cell RNA sequencing data are available at GEO of NCBI (GSE350516). Bulk RNA sequencing data of P5 and SD300 are available at SRA of NCBI (BioProject ID PRJNA1542153) . All data generated or analyzed during this study are included in this article (and its supplementary information files).

Code availability

Our custom single cell analysis pipeline is available at https://github.com/wsunjau/porcine-suspension-cell-state-analysis.

References

1. Van Eenennaam, A.L. Addressing the 2050 demand for terrestrial animal source food. *Proc Natl Acad Sci U S A* **121**, e2319001121 (2024).
2. Turk, J. Meeting projected food demands by 2050: Understanding and enhancing the role of grazing ruminants. *Journal of Animal Science* **94**, 53-62 (2016).

3. Post, M.J. *et al.* Scientific, sustainability and regulatory challenges of cultured meat. *Nature Food* **1**, 403-415 (2020).

4. Pelton, R.E.O. *et al.* Greenhouse gas emissions in US beef production can be reduced by up to 30% with the adoption of selected mitigation measures. *Nature Food* **5**, 787-797 (2024).

5. Gu, H. *et al.* Scaling Cultured Meat: Challenges and Solutions for Affordable Mass Production. *Comprehensive Reviews in Food Science and Food Safety* **24**, e70221 (2025).

6. Jara, T.C. *et al.* Stem cell-based strategies and challenges for production of cultivated meat. *Nature Food* **4**, 841-853 (2023).

7. Goodwin, C.M., Aimutis, W.R. & Shirwaiker, R.A. A scoping review of cultivated meat techno-economic analyses to inform future research directions for scaled-up manufacturing. *Nature Food* **5**, 901-910 (2024).

8. Muller, Q. & Matsusaki, M. Comparative analysis of cultivated meat cell sources and cell type usage across species: Functional roles and engineering potential. *Trends in Food Science & Technology* **169**, 105524 (2025).

9. Lee, J. *et al.* Optimizing muscle satellite cell sources for cultured meat: anatomical origin influences cellular properties and quality attributes. *npj Science of Food* **10**, 56 (2026).

10. Jeong, I. *et al.* Production of alternative fat from adipose-derived stem cell from bovine in 3D culture. *Applied Sciences* **15**, 7333 (2025).

11. Martins, B. *et al.* Advances and challenges in cell biology for cultured meat. *Annual review of animal biosciences* **12**, 345-368 (2024).

12. Stout, A.J. *et al.* Immortalized Bovine Satellite Cells for Cultured Meat Applications. *ACS Synthetic Biology* **12**, 1567-1573 (2023).

13. Pasitka, L. *et al.* Spontaneous immortalization of chicken fibroblasts generates stable, high-yield cell lines for serum-free production of cultured meat. *Nature Food* **4**, 35-50 (2023).

14. Hauser, M., Zirman, A., Rak, R. & Nachman, I. Challenges and opportunities in cell expansion for cultivated meat. *Frontiers in Nutrition* **11**, 1315555 (2024).

15. Pasitka, L. *et al.* Spontaneous immortalization of bovine fibroblasts following long-term expansion offers a non-transformed cell source for cultivated beef. *Nature Food* **6**, 1079-1094 (2025).

16. Thrower, T., Riley, S.E., Lee, S., Esteves, C.L. & Donadeu, F.X. A unique spontaneously immortalised cell line from pig with enhanced adipogenic capacity. *npj Science of Food* **9**, 52 (2025).

17. Gillio-Meina, C., Swan, C.L., Crellin, N.K., Stocco, D.M. & Chedrese, P.J. Generation of stable cell lines by spontaneous immortalization of primary cultures of porcine granulosa cells. *Molecular Reproduction and Development: Incorporating Gamete Research* **57**, 366-374 (2000).

18. Quek, J.P. *et al.* Exploring cost reduction strategies for serum free media development. *npj Science of Food* **8**, 107 (2024).

19. Stout, A.J. *et al.* Simple and effective serum-free medium for sustained expansion of bovine satellite cells for cell cultured meat. *Communications Biology* **5**, 466 (2022).

20. Skrivergaard, S., Krøyer Rasmussen, M., Sahebekhtiari, N., Feveile Young, J. & Therkildsen, M. Satellite cells sourced from bull calves and dairy cows differs in proliferative and myogenic capacity – Implications for cultivated meat. *Food Research International* **173**, 113217 (2023).

21. Pasitka, L. *et al.* Empirical economic analysis shows cost-effective continuous manufacturing of cultivated chicken using animal-free medium. *Nature Food* **5**, 693-702 (2024).

22. Kirsch, M., Morales-Dalmau, J. & Lavrentieva, A. Cultivated meat manufacturing: Technology, trends, and challenges. *Engineering in Life Sciences* **23**, e2300227 (2023).

23. Zhou, H. *et al.* Cost-effective production of meaty aroma from porcine cells for hybrid cultivated meat. *Food Chemistry* **473**, 142946 (2025).

24. Guo, R. *et al.* Serum-free long-term expansion and functional maintenance of pig satellite cells via targeted genetic engineering for cultured meat. *Food Materials Research* **5**, e007 (2025).

25. Liu, Z. *et al.* Engineering a genomically stable porcine myogenic cell line for serum-free cultured meat production. *Food Research International* **236**, 119134 (2026).

689 26. Messmer, T. *et al.* Single-cell analysis of bovine muscle-derived cell types for
690 cultured meat production. *Frontiers in Nutrition* **10**, 1212196 (2023).
691 27. Uezumi, A., Fukada, S., Yamamoto, N., Takeda, S. & Tsuchida, K.
692 Mesenchymal progenitors distinct from satellite cells contribute to ectopic fat
693 cell formation in skeletal muscle. *Nat Cell Biol* **12**, 143-152 (2010).
694 28. Joe, A.W. *et al.* Muscle injury activates resident fibro/adipogenic progenitors
695 that facilitate myogenesis. *Nat Cell Biol* **12**, 153-163 (2010).
696 29. Dohmen, R.G.J. *et al.* Muscle-derived fibro-adipogenic progenitor cells for
697 production of cultured bovine adipose tissue. *npj Science of Food* **6**, 6 (2022).
698 30. Vincent, A., Stange, K., Louveau, I., Röntgen, M. & Dessauge, F. Myogenic
699 and adipogenic potential of porcine muscle satellite cells isolated by flow
700 cytometry. *Differentiation* **144**, 100871 (2025).
701 31. Zhang, X. *et al.* Seeding density-dependent fate divergence of muscle stem
702 cells revealed by single-cell RNA sequencing for cultured pork production.
703 *Food Research International* **233**, 117879 (2025).
704 32. Weinreb, C., Rodriguez-Fraticelli, A., Camargo, F.D. & Klein, A.M. Lineage
705 tracing on transcriptional landscapes links state to fate during differentiation.
706 *Science* **367**, eaaw3381 (2020).
707 33. Pan, Y. *et al.* Molecular dynamics of immortalized chicken fibroblasts from
708 adherent cultivation to carrier-free suspension culture. *Food Bioscience* **73**,
709 107716 (2025).

34. Bueno, M.J. *et al.* Essentiality of fatty acid synthase in the 2D to anchorage-independent growth transition in transforming cells. *Nature Communications* **10**, 5011 (2019).

35. Sawyer, B.T. *et al.* Targeting fatty acid oxidation to promote anoikis and inhibit ovarian cancer progression. *Molecular cancer research* **18**, 1088-1098 (2020).

36. Yuen, J.S.K., Jr. *et al.* Perspectives on scaling production of adipose tissue for food applications. *Biomaterials* **280**, 121273 (2022).

37. Song, W.-J., Liu, P.-P., Meng, Z.-Q., Ding, S.-J. & Li, H.-X. N-acetylcysteine promotes the proliferation of porcine adipose-derived stem cells during in vitro long-term expansion for cultured meat production. *Food Research International* **166**, 112606 (2023).

38. Humbird, D. Scale-up economics for cultured meat. *Biotechnology and bioengineering* **118**, 3239-3250 (2021).

39. Pierozan, C.R. *et al.* Factors affecting the daily feed intake and feed conversion ratio of pigs in grow-finishing units: the case of a company. *Porcine health management* **2**, 7 (2016).

40. Zhu, H. *et al.* Production of cultured meat from pig muscle stem cells. *Biomaterials* **287**, 121650 (2022).

41. Liu, Y. *et al.* Engineered meatballs via scalable skeletal muscle cell expansion and modular micro-tissue assembly using porous gelatin micro-carriers. *Biomaterials* **287**, 121615 (2022).

42. Zhang, M. *et al.* Determination of multiple risk substances in cultured meat biomass and washing solutions using LC-MS/MS: method development, validation, and risk assessment. *Food Research International*, 119347 (2026).

43. Ong, K.J. *et al.* Food safety considerations and research priorities for the cultured meat and seafood industry. *Comprehensive reviews in food science and food safety* **20**, 5421-5448 (2021).

44. Zhao, L. *et al.* Obesity Impairs Embryonic Myogenesis by Enhancing BMP Signaling within the Dermomyotome. *Advanced Science* **8**, 2102157 (2021).

45. Chen, L. *et al.* Dynamic 3D genome reorganization during development and metabolic stress of the porcine liver. *Cell discovery* **8**, 56 (2022).

46. Feng, L. *et al.* The Landscape of Accessible Chromatin and Developmental Transcriptome Maps Reveal a Genetic Mechanism of Skeletal Muscle Development in Pigs. *International Journal of Molecular Sciences* **24**, 6413 (2023).

47. Zhang, Y. *et al.* Comparative Transcriptome Analysis Provides Insight into Spatio-Temporal Expression Characteristics and Genetic Regulatory Network in Postnatal Developing Subcutaneous and Visceral Fat of Bama Pig. *Frontiers in Genetics* **13**, 844833 (2022).

48. Ren, Z. *et al.* Integrated ATAC-seq and RNA-seq Analysis of In Vitro Cultured Skeletal Muscle Satellite Cells to Understand Changes in Cell Proliferation. *Cells* **13**, 1031 (2024).

753 49. Zhu, G. *et al.* Generation of three-dimensional meat-like tissue from stable pig
754 epiblast stem cells. *Nature Communications* **14**, 8163 (2023).
755 50. Zhang, P. *et al.* Comparative Transcriptomic Profiles of Differentiated
756 Adipocytes Provide Insights into Adipogenesis Mechanisms of Subcutaneous
757 and Intramuscular Fat Tissues in Pigs. *Cells* **11**, 499 (2022).
758 51. Yang, L., Wu, Z., Zhu, H., Ding, S. & Zhou, G. A method for evaluating the
759 degree of Adipogenic differentiation of porcine cells cultured in suspension
760 based on deep learning. *Food Research International* **212**, 116324 (2025).
761 52. Zhang, R.G., Wang, X.W., Yuan, J.H., Guo, L.X. & Xie, H. Using a
762 non-radioisotopic, quantitative TRAP-based method detecting telomerase
763 activities in human hepatoma cells. *Cell Research* **10**, 71-77 (2000).
764 53. Herbert, B.-S., Hochreiter, A.E., Wright, W.E. & Shay, J.W. Nonradioactive
765 detection of telomerase activity using the telomeric repeat amplification
766 protocol. *Nature protocols* **1**, 1583-1590 (2006).
767 54. Vallabhaneni, H. *et al.* High basal levels of γH2AX in human induced
768 pluripotent stem cells are linked to replication-associated DNA damage and
769 repair. *Stem Cells* **36**, 1501-1513 (2018).
770 55. Jiang, H. *et al.* Effect of cell-cultured pork biomass on the texture and flavor
771 characteristics of plant-based meat analogues. *Food Bioscience* **74**, 107875
772 (2025).
773
774
775 **Acknowledgement**

This study was supported by the Agricultural Science and Technology Major Project, the Nanjing Major Science and Technology Special Project (Comprehensive Category, 202309014), the 2024 Central Government Guidance Fund for Local Science and Technology Development (Key Core Agricultural Technology Research and Achievement Transformation, BE2024007), and the Jiangsu Agricultural Science and Technology Innovation Fund (CX (24)1019).

Author contributions

Conceptualization by G.Z, S.D., and L.Z. funding by G.Z, S.D. Investigation by L.Z., S.D. Methodology by H.L., H.Z., Z.W., Y.K., B.Y., C.J., C.W., W.L., Y.X. Resources by S.D., C. L., C.T. Writing by L.Z, H.L, and S.D.

Competing interests

H.L., H.Z., Z.W., Y.K., B.Y., C.J., C.W., W.L., and S.D. are employees of Joes Future Food Technology Co. Ltd, which developed the cell line and the culture media and participated in this study. All authors declare no other competing interests.

Figures

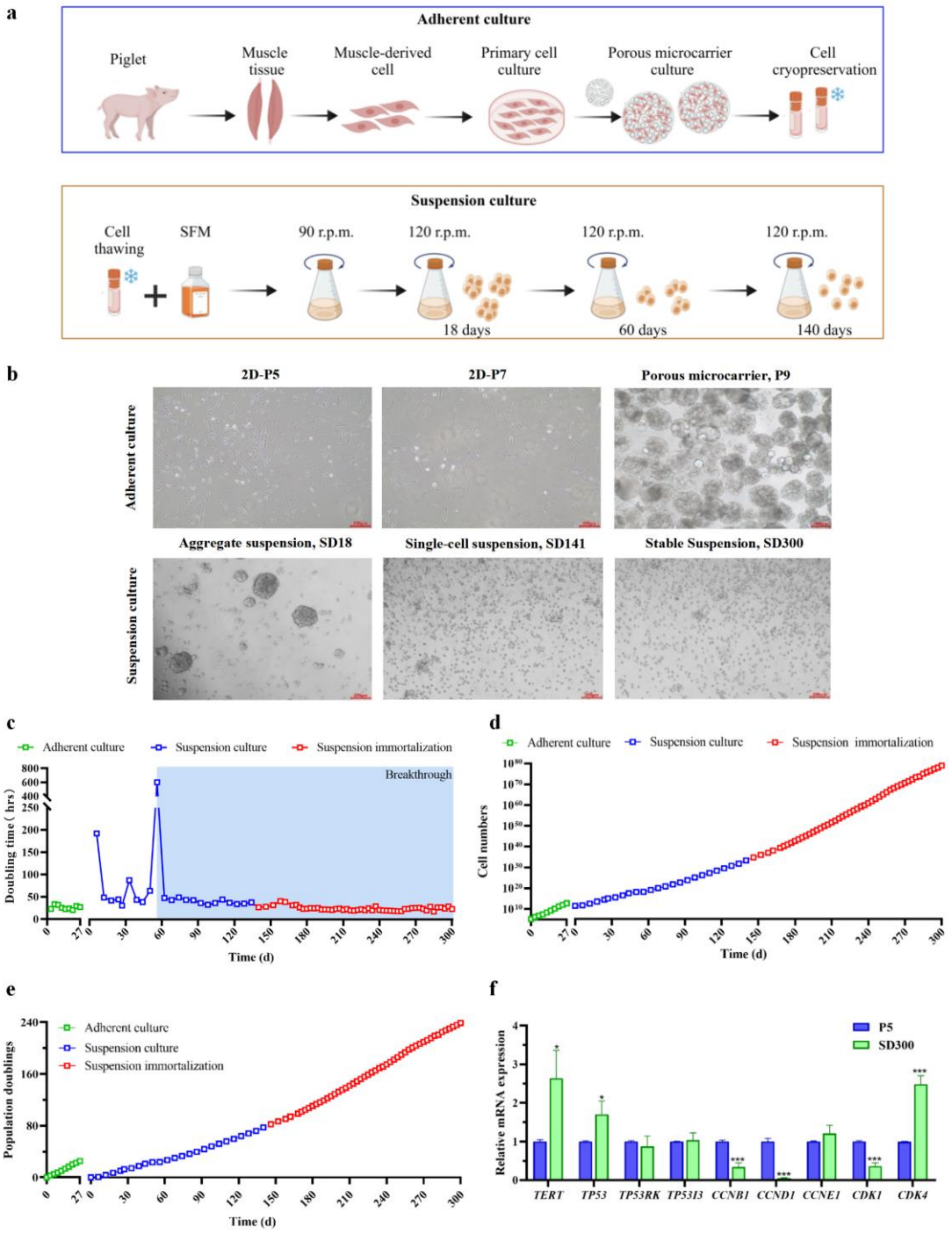


Fig. 1 | Establishment of a spontaneously immortalized porcine muscle-derived cell line through serum-free suspension adaptation.

a, Schematic of cell isolation, adherent expansion, cryopreservation and suspension adaptation. b, Representative phase images of cells at the indicated stages. Scale bars, 200 μm. c, Population-doubling time. d, Theoretical cumulative cell number. e, Cumulative population doublings (PDs). f, Relative gene expression in P5 and SD300 cells. Data are mean ± SD; n = 3. ***$P < 0.001$. P, passage; SD, suspension day. Images in part a were created with BioGDP.com.

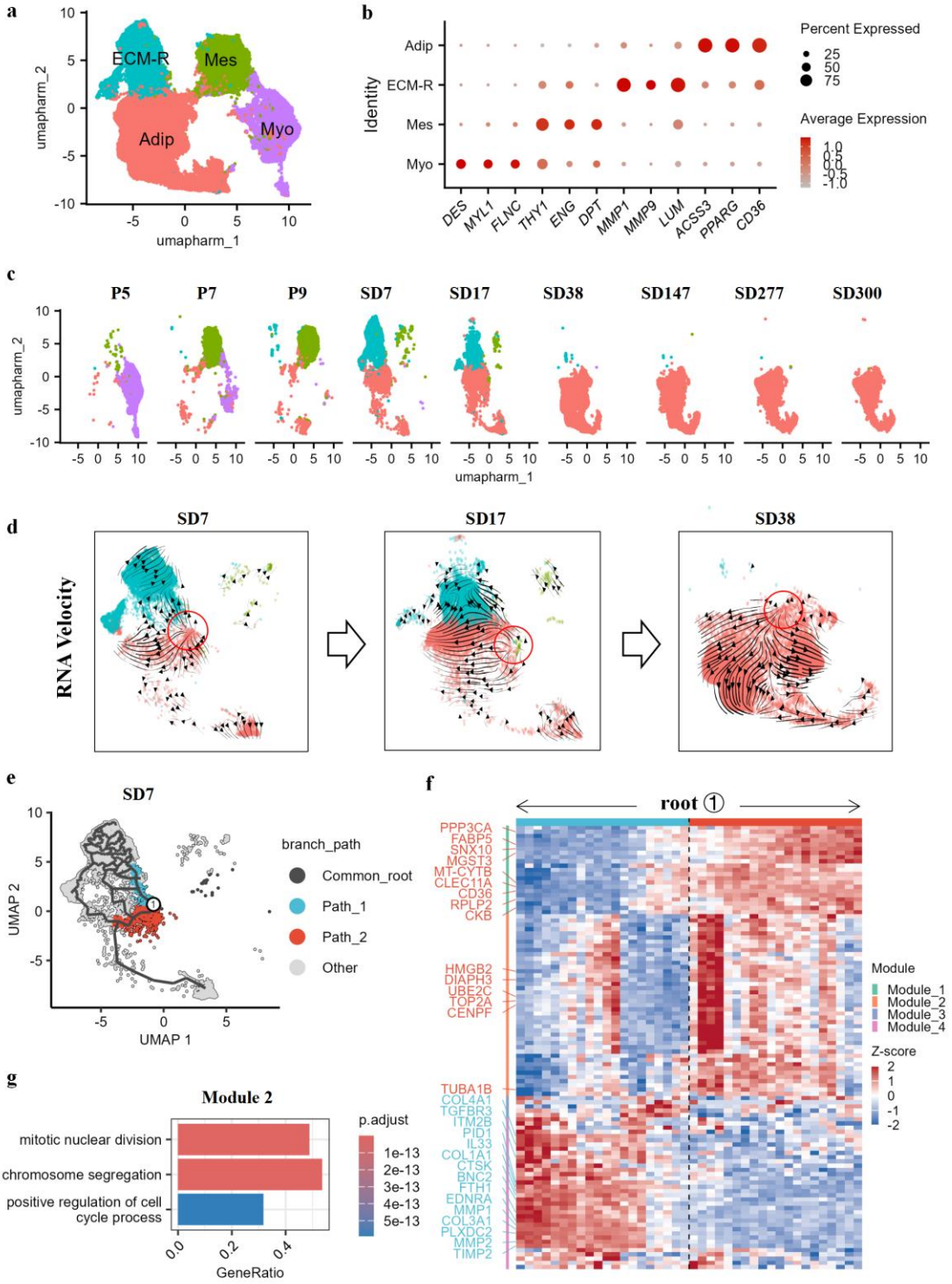


Fig. 2 | Cell-state remodelling and transcriptional trajectories during serum-free suspension adaptation analyzed by scRNA-seq.

a, Uniform manifold approximation and projection (UMAP) of the integrated single-cell RNA-sequencing dataset, coloured by transcriptional state: myogenic (Myo), mesenchymal stromal-like (Mes), extracellular matrix-remodelling (ECM-R) and adipogenic-like (Adip). b, Expression of representative marker genes. c, UMAPs separated by culture stage, spanning adherent expansion (P5 and P7), microcarrier

culture (P9) and suspension culture (SD7 - SD300). Colours correspond to the states in a. d, RNA-velocity streamlines projected onto UMAPs at SD7, SD17 and SD38. Streamlines indicate inferred directions of transcriptional change, and red circles highlight regions of local divergence. e, Selected pseudotime paths at SD7 originating from a shared root (①). f, Heatmap of gene-expression dynamics along the two paths in e, grouped into four modules. g, Selected Gene Ontology biological processes enriched among Module 2 genes. P, passage; SD, suspension day.

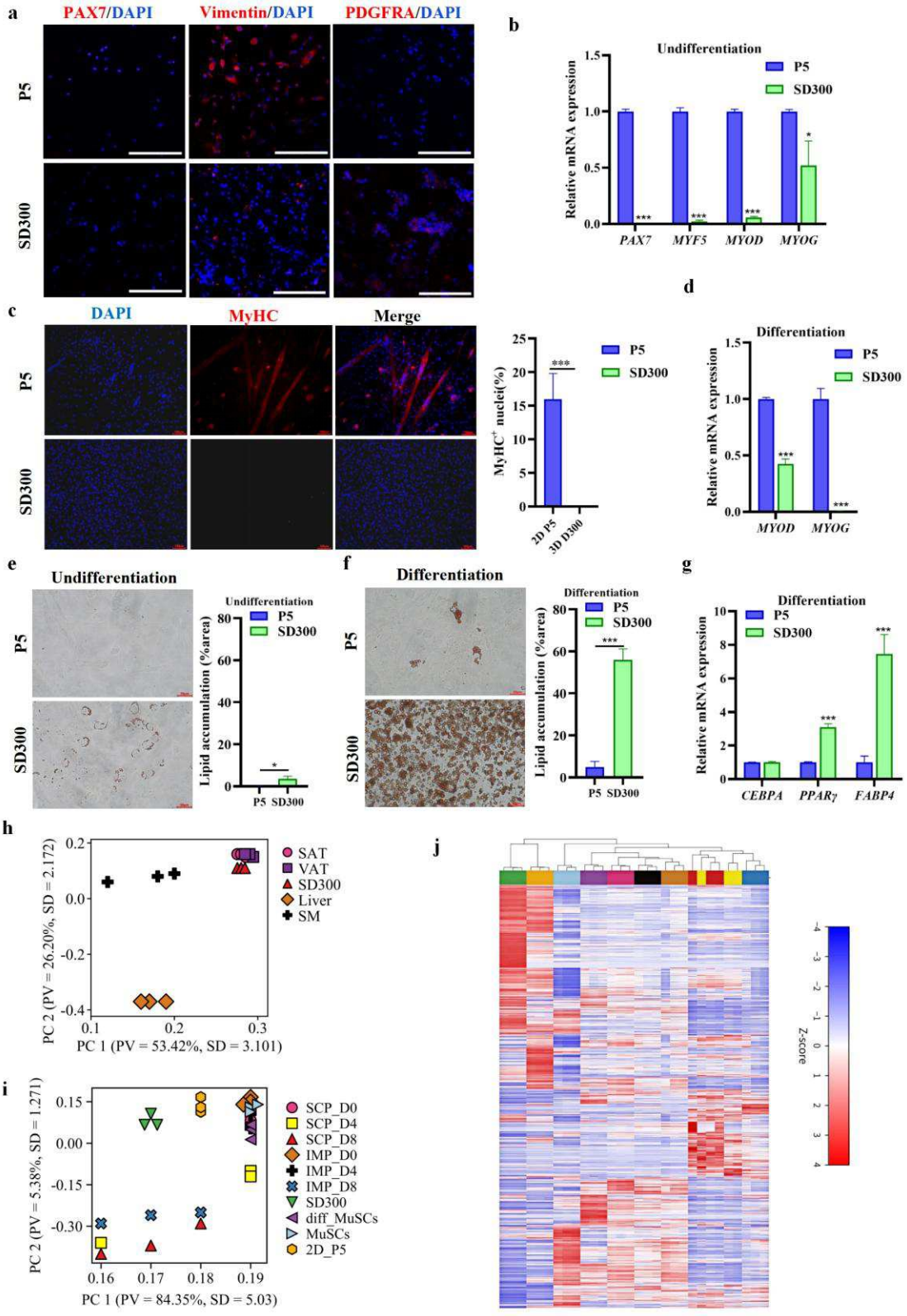


Fig. 3 | Loss of myogenic potential and acquisition of adipogenic features after long-term suspension culture.

a, Immunofluorescence staining of PAX7, vimentin and PDGFRA in parental P5 cells and SD300 cells replated under adherent conditions. Nuclei were counterstained with DAPI. b, Relative mRNA expression under non-inducing conditions. c, Myosin heavy

chain (MyHC) immunofluorescence and quantification of the differentiation index after myogenic induction. d, Relative mRNA expression after myogenic induction. e,f, Oil Red O staining and quantification of the stained area (%) under non-inducing conditions (e) and after adipogenic induction (f). g, Relative mRNA expression after adipogenic induction. h, Principal component analysis (PCA) comparing SD300 transcriptomes with reference bulk RNA-seq datasets from porcine skeletal muscle, liver, and subcutaneous and visceral adipose tissues. i, PCA comparing SD300 and parental P5 cells with primary porcine myogenic and adipogenic reference populations at different stages of differentiation. j, Heatmap of gene-expression profiles across cell populations in i. Data are mean ± SD; n = 3. Scale bars, 100 μm (a,c) and 50 μm (e, f). * $P < 0.05$, *** $P < 0.001$.

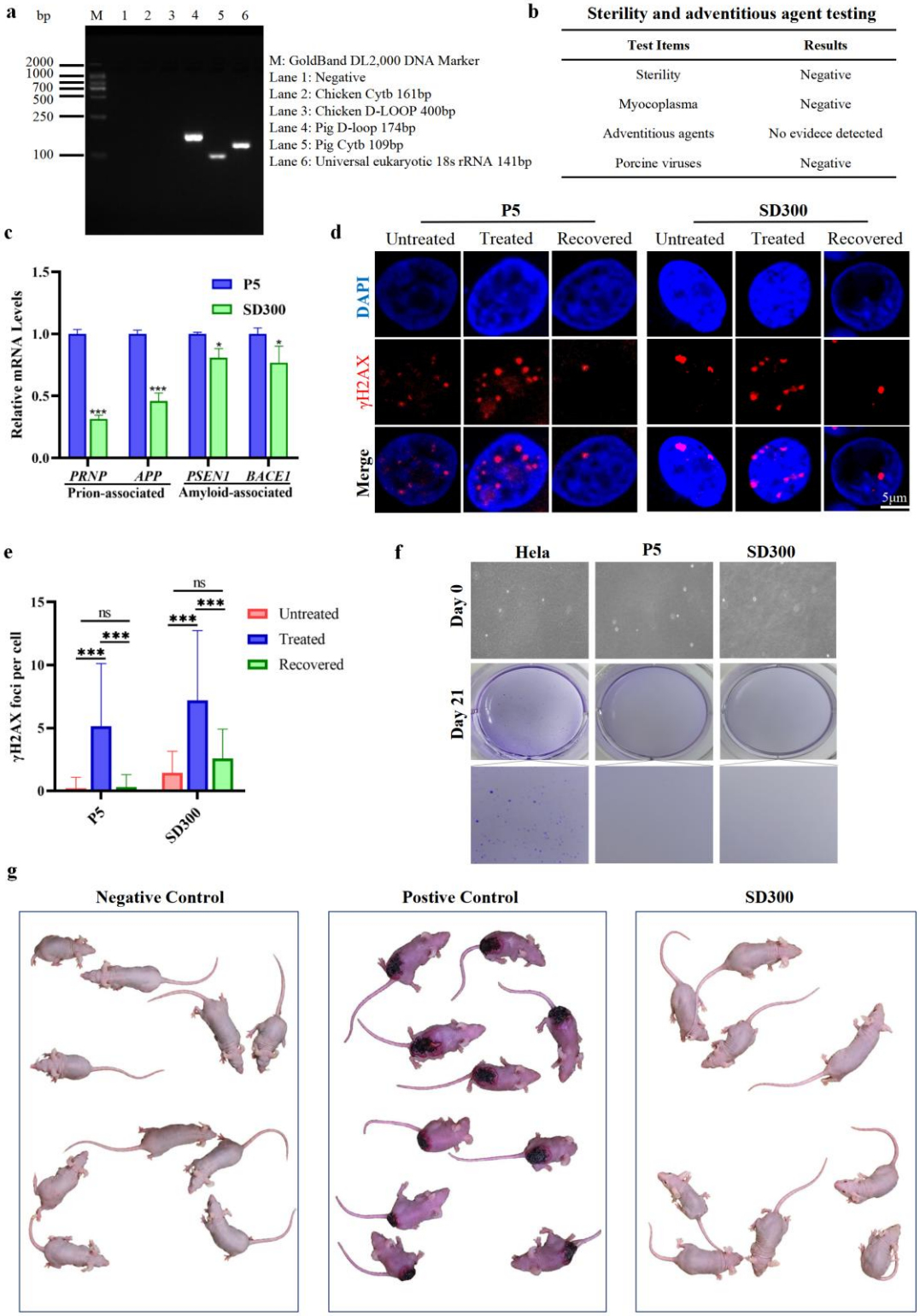
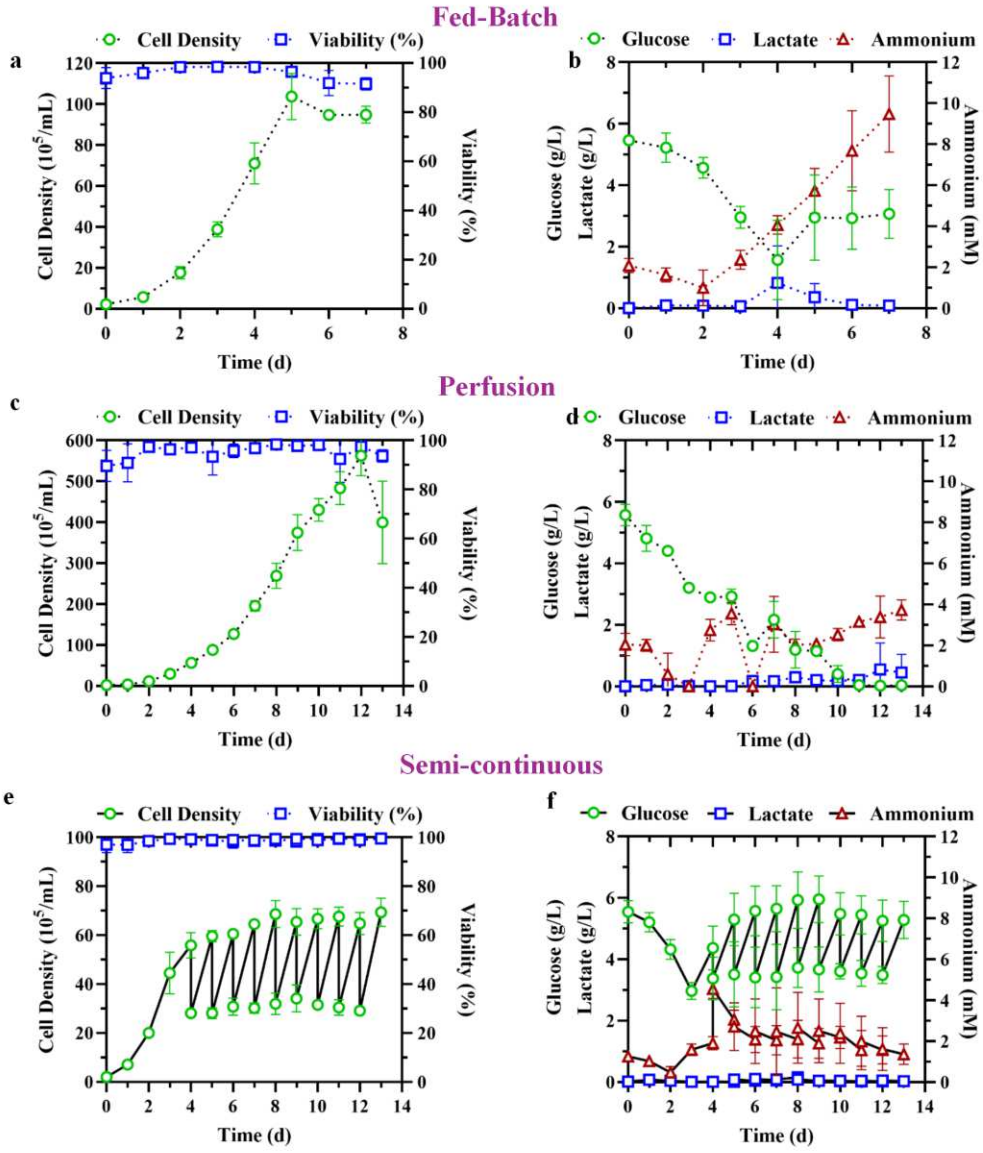


Fig. 4 | Species authentication and safety-related characterization of SD300 cells. a, PCR-based species authentication of SD300 cells. b, Summary of independent third-party sterility and adventitious-agent testing. The complete testing panel and results are provided in Extended Data Table 1. c, Relative mRNA expression of selected prion- and amyloid-related genes. d, Representative immunofluorescence

images of γH2AX (red) and DAPI-stained nuclei (blue) in P5 and SD300 cells under untreated conditions, after DNA-damage induction and following recovery. Scale bar, 5 μm. e, Quantification of γH2AX foci per cell. f, Soft-agar colony formation assay of HeLa, P5 and SD300 cells, showing initial cultures (day 0) and stained cultures after 21 d. HeLa cells served as a positive control. g, Endpoint images of mice in the negative-control, positive-control and SD300 groups in the in vivo tumorigenicity assay. Data are mean ± SD; n = 3 for c, f; n = 50 for e, n = 10 for g.



g

Summary of outcomes from three independent process

	Fed-batch	Perfusion	Semi-continuous
Seeding density	0.22±0.04E6/mL	0.21±0.03E6/mL	0.21±0.02E6/mL
Days	7	13	13
Max. cell density	10.37±1.13E6/mL	56.27±4.84E6/mL	6.94±0.58E6/mL
Medium volume	27.97±1.07L	12.38±0.24L	50.52±0.55L
Accumulated medium volume	33.85±1.22L	256.37±0.11L	287.18±10.95L
Medium dry weight	900.02±32.45g	3640.38±1.51g	5077.40±193.64g
Accumulated wet biomass	935.13±86.67g	1028.15±259.00g	6585.30±458.08g
Medium conversion ratio	0.96±0.07	3.54±0.81	0.77±0.02

Fig. 5 | Comparison of serum-free bioprocesses for porcine cell biomass production.

a,b, Viable cell density and viability (a) and metabolite concentrations (b) during fed-batch culture. c,d, Corresponding profiles during cell-retention perfusion. Perfusion was initiated at 0.5 vessel volumes per day (VVD) on day 3 and increased

to 2 VVD from day 5. e,f, Corresponding profiles during repeated harvesting, with the cell-containing outflow collected as ten consecutive 24-h harvest fractions. g, Comparison of process parameters, biomass output and medium conversion ratio across the three configurations. The medium conversion ratio was calculated as dry medium mass divided by wet biomass. Each configuration was tested in three independent production runs. Data are mean ± SD.

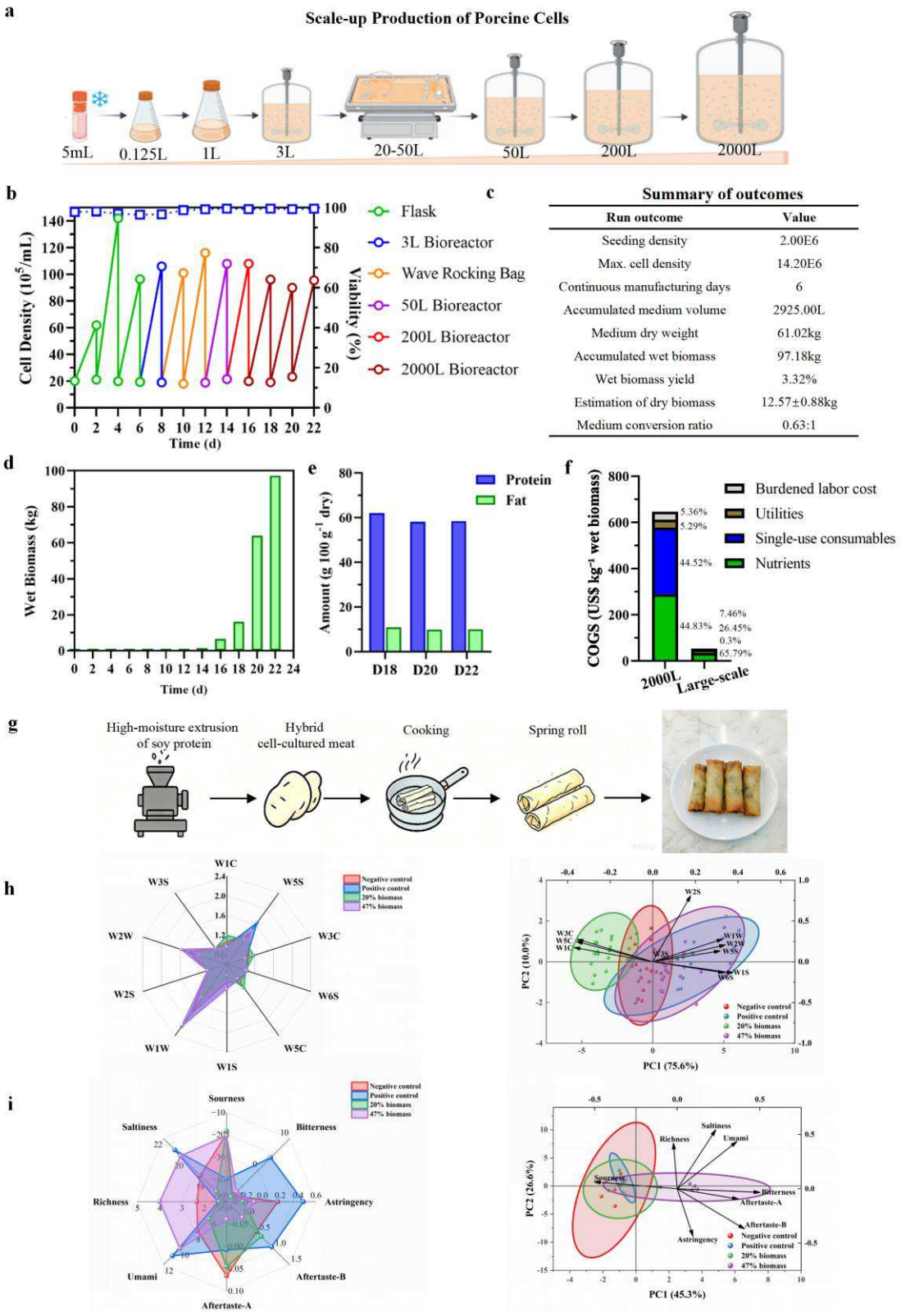


Fig. 6 | Scale-up of repeated-harvest culture and evaluation of the harvested biomass.

a, Schematic of seed-train expansion from a working-cell-bank to a 2,000-litre production vessel. b, Cell-density profiles during sequential expansion and repeated harvesting. c, Summary of process inputs and biomass output. The medium

conversion ratio was calculated as dry medium mass consumed divided by wet biomass produced. d, Cumulative wet biomass output. e, Protein and fat contents of biomass harvested on days 18, 20 and 22, expressed per 100 g of dry biomass. f, Estimated cost-of-goods (COGS) breakdown for the 2,000-litre process, a large-scale scenario and an industry forecast. g, Preparation workflow and representative images of hybrid spring rolls incorporating harvested cell biomass and high-moisture-extruded soy protein. h,i Electronic-nose (h) and electronic-tongue (i) response profiles (left) and principal component analysis biplots (right) for the negative control, positive control and formulations containing 20% or 47% cell biomass. Images in part a and g were created with BioGDP.com.

Supplementary Files

This is a list of supplementary files associated with this preprint. Click to download.

- Supplementarytable1.xlsx
- Supplementarytable3.xlsx
- Supplementarytable2.xlsx
- ExtendedData20261016zhao.docx
- Supplementarytable4.xlsx